Spectrochimica Acta Part A: Molecular and Biomolecular Spectroscopy, Volume 255, July 2021, Article number 119724
DOI:10.1016/j.saa.2021.119724

Molecular structure characterization of bituminous coal in Northern China via XRD, Raman and FTIR spectroscopy

Jingyu Jiang[a,b,c*], Shuo Zhang[a,b], Phil Longhurst[c], Weihua Yang[a,b], Shaojie Zheng[a,b]**

[a] *Key Laboratory of Gas and Fire Control for Coal Mines (China University of Mining and Technology), Ministry of Education, Xuzhou, 221116, China*

[b] *School of Safety Engineering, China University of Mining and Technology, Xuzhou, Jiangsu, 221116, China*

[C] *School of Water, Energy and Environment, Cranfield University, Bedford, MK43 0AL, UK*

* Corresponding author. School of Safety Engineering, China University of Mining and Technology, Xuzhou, Jiangsu 221116, China.

** Corresponding author. School of Water, Energy and Environment, Cranfield University, Bedford,MK43 0AL, UK.

E-mail addresses: jiangjingyu@cumt.edu.cn(J. Jiang), p.j.longhurst@cranfield.ac.uk (P. Longhurst).

Abstract:

Bituminous coal is used widely for a variety of applications despite causing a range of problems within processes. The complexity and heterogeneity of the molecular structure of coal is one of the reasons for problems during use. Investigation into the molecular structure of the bituminous coal is reported from using X-ray diffraction (XRD), Raman spectroscopy, and Fourier

Transform infrared spectroscopy (FTIR) experiments on four coal samples from northern China.

The average lateral sizes (L_a), stacking heights (L_c) and interlayer spacing (d_{002}) of the coal samples' crystallite structures derived from the XRD ranged from 25.78 to 27.93 Å, 17.27 to 25.88 Å and 3.40 to 3.52Å, respectively; and the G-D_1, I_{D1}/I_G and L_a of the samples ranged from 245.06 to 249.63cm^{-1}, 2.18 ~ 2.48 and 18.16 to 20.64 Å, respectively. The FTIR spectra reveals that coal samples incorporate oxygen-containing functional groups, aliphatic functional groups, aromatic functional groups and hydroxyl functional groups. Results show these four coal samples contained a low degree of ordered microcrystalline units with a low degree of aromatic conformation. The samples have the largest proportion of oxygenated functional groups, followed by aromatic structures, aliphatic structures and hydroxyl groups. Results from this study could inform the ongoing study of molecular structural characteristics of bituminous coal as well as help our understanding of properties such as wettability and pore structure.

Key words: Molecular structure; Bituminous coal; XRD; Raman spectroscopy; FTIR

1. Introduction

The coal industry is one of the pillars of the world's energy industry, as it provides abundant and widely distributed fossil energy resources for power generation [1]. There are notable difference in coal from ashless high calorific value material under constant humidity and volatile matter on dry ash free basis (V_{daf}), coal is roughly divided into lignite, bituminous coal and anthracite. Currently, bituminous coal is widely used in coking, power generation, coal gasification, fuel, and fuel cells because of its easy combustion, low ash and moisture content, and high calorific value. Coal is mainly a complex three-dimensional structure composed of fused aromatic moieties [2]. This highly complex substance composed of minerals that reflect the sedimentary environment and nature of organic precursors, complicates the characterization and utilization of coal samples [3]. By studying the molecular structure of bituminous coal, its processing and utilization technology can be improved, thus improving coal classification and quality measure for use. Many researchers have studied the molecular structure of coal through various spectroscopic techniques, such as XRD [4-5], NMR [6], TEM [7], Raman [8-9] and FTIR [6,9] spectroscopy. However, due to the heterogeneity and complexity of coal, many problems and difficulties in the detailed characterization of its molecular structure remain. In this study, X-ray diffraction (XRD), Raman spectroscopy and Fourier Transform Infrared (FTIR) spectroscopy were used to investigate the molecular structure of coal.

X-ray diffraction [XRD] is a non-destructive technique that can obtain the molecular pattern of a sample. The diffraction angle/direction characterizes the shape and size of the unit cell, and the intensity reflects the arrangement of atoms in the unit cell [10]. By analyzing the diffraction pattern, the structural parameters such as aromaticity (f_a), carbon stacking layer spacing (d_{002}), average lateral sizes (L_a), and stacking height of crystallite (L_c) of the carbon accumulation structure can be calculated [11-12]. Since observation of the Raman Effect in 1928, Raman spectroscopy has been widely used in the characterization of carbonaceous materials, with techniques and analytical methods becoming more mature. The Raman spectrum of carbonaceous materials can be divided into first order and second order [13]. For graphite, there is only one band around 1580cm^{-1}, which we called G band. While the study found that for highly disordered carbon, peak bands induced by micro-lattice defects appear at 1150, 1350, 1530 and 1620 cm^{-1} in the first-order region [14-15]. And the intensity ratio of D1 and G band and the full width at half maximum (FWHM) of the G band has been proven to assess

the crystallinity and degree of order of the carbonaceous material [16-17]. Fourier transform infrared (FTIR) spectroscopy can be used to study and analyse the functional group composition of coal, and then to understand the molecular structure of coal [18-19]. This technology reveals the hydrocarbon structure including the aromatic and aliphatic, and heteroatomic functions (mainly oxygenated), and is one of the most powerful coal characterization technologies at present [20]. The data obtained by FTIR can calculate parameters such as f_a, (R/C) u, Hal/H and CH_2/CH_3, which can be used to quantitatively analyse the functional group composition and aromaticity of coal.

In summary, the reserves of bituminous coal account for a relatively large proportion in China, and its utilization still has great potential, but current research on the molecular structure of bituminous coal is incomplete because of our understanding of the heterogeneity and diversity of coal. Therefore, in this paper, XRD, Raman and FTIR spectroscopy techniques were applied to analyse the molecular structure of three groups of bituminous coal samples and a sub-bituminous coal sample which serve as comparative samples.

2. Coal samples and experiment methods

2.1 Coal samples

According to the large storage of bituminous coal in northern China, in this work, three bituminous samples were collected from coal mines of Daxing, Xiaoqing in Liaoning province and Xinyi in Henan province in China, which are coded as TFXQ, TFDX and YMXY, respectively in this study. A comparative sub-bituminous coal sample is from coal mine Puhe in Liaoning province in China, which is marked as SBPH. These samples were demineralized before XRD, Raman and FTIR spectroscopy experiments, which can reduce the amount of minerals in order to improve the accuracy of quantitative analysis [21].

2.2. Proximate and ultimate analysis

Ultimate analysis was performed according to the international standard ISO 11722:2013 and ISO 1171: 2010. Proximate analysis was carried out in accordance with ISO 17247: 2013 and ISO 19579: 2006. The Ro was measured under polarized conditions by a microscope photometer (Zeiss, Germany) according to international standards ISO 7404-5:1984.

Parameters, such as the apparent aromaticity (f_a), the ratio of aliphatic hydrogen (Hal) to total

hydrogen atoms (H) H_{al}/H and the number of the rings of aromatic carbon in the monomer $(R/C)_u$,can be calculated from the data of proximate analysis and ultimate analysis. To characterize aromaticity, Mielczarski et al. proposed f_a which can be calculated according to the Eq. (1).

$$f_a = (100 - VM) \times 0.9677/C \quad (1)$$

where VM represents volatiles matter and C is the carbon content. 0.9677 is the fitting coefficient [22]. $(R/C)_u$ represents the number of rings of aromatic carbon in the monomer, which can be calculated according to the Eq. (2) proposed by Kastner[23].

$$(R/C)_u = 1 - \frac{f_a}{2} - \frac{(H/C)}{2} \quad (2)$$

where Hal/H represents the ratio between the concentrations of aliphatic (Hal) and the total hydrogen atoms (H), which can be calculated by Eq. (3)[24]:

$$H_{al}/H = (1 - f_a)/(C_{al}/H_{al})/(H/C) \quad (3)$$

where C_{al}/H_{al} value is the atomic ratio between C and H in aliphatic groups, which is known to be about 5.5 for coals.

2.3. X-ray diffraction analysis

The XRD experiment was performed by the D8 ADVANCE X-ray diffractometer manufactured by Bruker, Germany and CuKα radiation (40kV, 30mA). Detailed experimental conditions are as follows. Ni fillers were used to filter out Cu-Kβ radiation. Besides, DS (Divergence Slit) and SS(Anti-scatter silt) were 0.6mm and 8mm respectively. Detector opening was 2.82°, while Primary soller slit and Secondary soller slit were both 2.5°. Powdered samples were scanned from 3°~75° in 2θ range with 0.019450° step interval and 0.2sec/step counter-time. Origin 2017 software was used to denote the XRD spectrum. The broad hump was fitted to three Gaussian peaks around 20°, 26°and42°, representing γ peak, 002 peak and 100 peak respectively. The peak position (θ), intensity (I), area (A) and full width at half maximum(β) were determined by XRD spectrum. The number of aromatic carbon atoms (C_{ar}) and aliphatic carbon atoms (C_{al}) are equal to the areas under 002 peak and γ peak respectively [9, 25, 26]. Therefore, the aromaticity(f_a) which is the radio of carbon atoms in aromatic rings, can be calculated by the Eq.(4)[4]:

$$f_a = C_{ar}/(C_{ar} + C_{al}) = A_{002}/(A_{002} + A_\gamma) \quad (4)$$

where A_{002} and A_γ are the areas of the 002 peak and the γ peak, respectively. The lateral size (L_a) which

provides the in-plane dimension of crystalline carbon and the staking height (L_c) contributes the height of the crystalline carbon can be obtained by Debye-Scherrer Eqs.(5-6). The d_{002} can be calculated by Braggs Eq. (7).

$$L_a = 1.84\lambda/(\beta_{002}\, cos\theta_{002}) \quad (5)$$

$$L_c = 0.89\lambda/(\beta_{100}\, cos\theta_{100}) \quad (6)$$

$$d_{002} = \frac{\lambda}{2sin\theta_{002}} \quad (7)$$

where λ represents the wavelength of the X-ray(γ=0.15405nm), β_{002} and β_{100} are the FWHM (full width at half maximum) of the 002 peak and the 100 peak, respectively. The θ_{002} and θ_{100} are the diffraction angles corresponding to the peak positions of 002 peak and 100 peak.

2.4. Raman spectroscopy analysis

Raman measurement was carried out to study the changes in the molecular structure, using a Senterra Raman spectrometer produced by Bruker, Germany at room temperature. The experiment was completed at the Modern Analysis and Computing Center of China University of Mining and Technology. Samples were demineralized and ground into powder (200 mesh) before measuring molecular parameters with a laser confocal Raman spectrometer. Equipped with a 532 nm laser, a laser power of 5 mW, a resolution of 9–18 cm^{-1}, an integration time of 2 s, a cumulative number of 10 times was used. The spectral resolution is less than or equal to 1.5 cm-1, lateral resolution is less than 1 mm, longitudinal resolution is less than 2 mm, and the excitation wavelengths are 785 nm, 633 nm, and 532 nm, respectively. Applying Origin 2017 to fit Raman spectral peaks between 1000 and 2000 cm^{-1}. We obtained the intensity(I), peak position(θ) and full width at half maximum (FWHM). The microcrystalline planar crystalline size L_a can be calculated by Eq.(8)[27]:

$$L_a = C(\lambda_L)[I_D/I_G]^{-1} \quad (8)$$

where λ_L is the wavelength of Raman laser, C (λ_L) is the wavelength pre-factor, I_D and I_G are the intensity of the D and G bands respectively. C (λ_L) . This can be calculated by Eq. (9):

$$C(\lambda_1) = C_0 + \lambda_L C_1 \quad (9)$$

where C_0=−12.6 nm, and C_1=0.033.

2.5. FTIR spectroscopy analysis

To study the molecular structure and its chemical bond it is necessary to use FTIR spectroscopy.

This determines the molecular bond length, infers the three-dimensional configuration of the molecule, and determines the organic functional group composition in the sample. The FTIR experiment was conducted at the Modern Analysis and Computing Center of China University of Mining and Technology by a TIR Vertex 80v infrared spectrometer manufactured by Bruker, Germany. The coal sample, which had been abraded into powder and demineralized, was scanned 32 times in the wavenumber range of 4000–400 cm^{-1} with a spectral resolution of 8 cm^{-1}. Origin 2017 software was used to fit the peaks of the spectrum map. Infrared spectrum fitting peaks provides key information on the relative concentrations of aromatic carbons (C_{ar}), aliphatic carbons (C_{al}), and carbonyl (C=O) groups etc. [28]. The apparent aromaticity (fa) can be calculated by Eq. (10-14):

$$Har = \frac{A_{ar}}{a_{ar}} \tag{10}$$

$$Hal = \frac{A_{al}}{a_{al}} \tag{11}$$

$$\frac{H_{al}}{H} = \frac{H_{al}}{H_{al}+H_{ar}} = \frac{A_{2800-3000}}{A_{2800-3000}+A_{700-900}} \tag{12}$$

$$\frac{C_{al}}{C} = \left(\frac{H_{al}}{H} \times \frac{H}{C}\right) \Big/ \frac{H_{al}}{C_{al}} \tag{13}$$

$$f_a = 1 - \frac{C_{al}}{C} \tag{14}$$

where A_{ar} and A_{al} are the integral areas of absorbance in the aromatic hydrogen (900-700 cm^{-1}) and aliphatic hydrogen (3000-2700 cm^{-1}) bands, respectively; a_{ar} and a_{al} (extinction coefficients) are used to convert the integral area of absorbance to concentration content. For lignite and sub-bituminous coal, the a_{ar} is 541 cm^{-1} and the a_{al} is 710 cm^{-1}. Hal/H is the ratio between the concentrations of aliphatic (H_{al}) and the total hydrogen atoms (H), H_{ar} is the aromatic hydrogen, H/C is the ratio of hydrogen atoms to carbon atoms, calculated from the ultimate analysis, $A_{2800\text{-}3000}$ and $A_{700\text{-}900}$ are integrated absorbance band areas at 2800–3000cm^{-1} and 700-900cm^{-1}. The aliphatic structural parameter $A(CH_2)/A(CH_3)$ is calculated by Eq. (15) [28]:

$$\frac{A(CH_2)}{A(CH_3)} = \frac{A_{2935-2919}}{A_{2975-2950}} \tag{15}$$

3. Results and discussion

3.1. Coal chemical properties of bituminous coal

According to Eqs.(1)-(3), the proximate and ultimate analyses results are shown in Table 1. Industrial analysis (M, A, VM, FC) of these samples were performed according to GB/T 476-2008, GB/T

212-2008 and GB/T 483-87. The ranges of the parameters fa, (R/C)u, H_{al}/H are 0.78-0.96, 0.49-0.57, and 0.06-0.55, respectively.

Table 1 Proximate and ultimate analyses results

Sample	Proximate analysis (wt.%)				Ultimate analysis (wt.%)					H/C	R_O (%)	f_a	$(R/C)_u$	H_{al}/H
	M	A	VM	FC	C	H	O	N	S					
SBPH	15.12	19.12	42.50	23.26	71.49	5.23	17.53	4.05	0.49	0.88	0.43	0.78	0.57	0.55
TFXQ	8.43	36.09	28.04	27.44	68.18	4.98	15.35	2.03	0.47	0.88	0.57	0.93	0.50	0.17
TFDX	5.23	19.46	30.17	45.14	70.65	5.01	14.11	1.69	0.53	0.85	0.70	0.96	0.49	0.10
YMXY	3.03	5.98	20.67	72.32	90.04	4.05	7.33	1.37	2.88	0.54	1.09	0.85	0.55	0.06

M: moisture; A: ash, on a dry basis; VM: volatile matter, on dry ash free (daf) basis; FC: fixed carbon (daf basis); all ultimate analyses reported on a daf basis except sulfur on a dry basis; R_o: mean random vitrinite reflectance (%, oil).

It can be seen from the table that the results of the industrial analysis of the four coal samples are quite different, the range of moisture (M) is 3.03~15.12%, the range of ash (A) is 5.98~36.09, the range of volatile fraction (VM) is 20.67~42.50% and the range of fixed carbon (FC) is 23.26~72.32%, among which the fixed carbon content of SBPH, TFDX and TFXQ samples is low, while the fixed carbon content of the meager coal sample YMXY is significantly higher than other samples. Elemental analysis of the four coal samples showed that the elemental content of the coal samples was dominated by C elements, followed by O and H elements, with N and S elements accounting for a very small proportion. The residual element content varies greatly between the coal samples, except for the H element, which varies little. The content range of element C is 68.18~90.04%, H is 4.05~5.23%, O is 7.33~17.53, N is 1.37~4.05, S is 0.47~2.88%, and R_O is 0.43~1.09%. TFDX, TFXQ and YMXY belong to bituminous coal (medium rank coal) while SBPH belongs to sub-bituminous coal (low rank coal), according to the international standard ISO 11760:2005.

3.2. X-ray diffraction analysis

Fig. 1 shows the X-ray diffraction spectra of the four groups of coal samples used in the experiment. It can be seen that each coal sample has basically the same characteristics and all show high background intensity, which indicates that the coal sample contains a highly disordered material with a definite proportion of amorphous carbon form. There are two clear peaks in the figure, and the corresponding diffraction angles are located at about 26 ° and 47 °, respectively, which are 002 and 100 peaks. The 002 band shown in the figure relates to the stacking between the aromatic ring layers

199 which corresponds to the ordinary crystallites formed by poly-condensation of the aromatic core, i.e.
200 the aromatic crystallites. The γ band which located at the left side of the 002 peak is caused by
201 aliphatic hydrocarbon branches, various functional groups, and alicyclic hydrocarbons, called branched
202 crystallites, which are connected to the poly-condensation aromatic core.

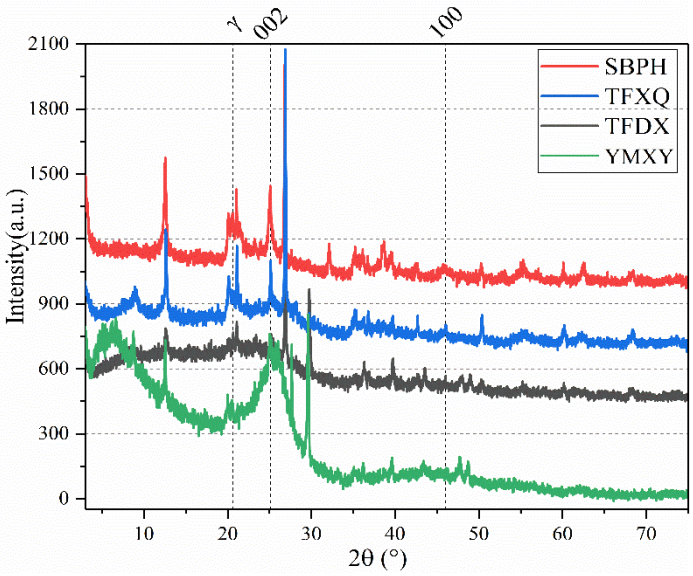

203
204 Fig. 1 The XRD spectra of four coal samples

205 Due to the stacking of peaks, we used Origin 2017 to perform split-peak fitting of peaks from 5° to
206 35°, resulting in two Gaussian peaks, 002 and γ, which were fitted near 20° and 26°, respectively, to
207 obtain information on the corresponding parameters such as peak position, area, half-height and
208 width. Fig. 2 shows the fitting curve of the TFXQ coal sample at 5 to 35°.

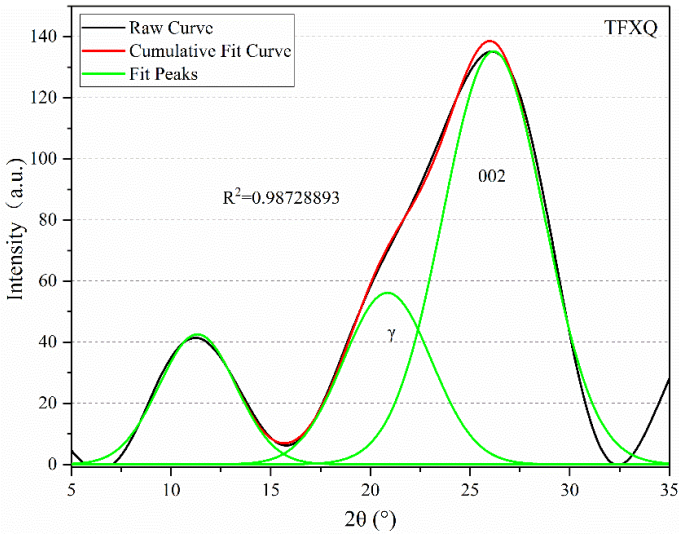

209
210 Fig. 2 Gaussian fitting curve of γ peak and 002 peak of TFXQ coal sample in 2θ range of 5-35°
211 From the results of peak fitting, we can obtain the area of the 002 peak and γ peak, and thus the

sample parameters d_{002}, f_a, L_c and L_a can be calculated using Eqs. ((4)-(7)). The results are shown in Table 2. The range of d_{002} can be found to be 3.40 to 3.52 Å, indicating that the coal samples contains a low degree of ordered microcrystalline units relative to pure graphite (3.36 to 3.37 Å). The range of parameter aromaticity f_a is 0.62 to 0.91. L_c and L_a reflects both the lamellar ductility and stacking of the microcrystals with values ranging from 17.27 to 25.88 Å and 25.78 to 27.93 Å, respectively. The aromatization of bituminous coal is not generally high. The TFXQ and YMXY coals have higher aromaticity f_a among the four samples, and their L_a and L_c values are relatively large. This also implies that the microcrystalline size is correspondingly larger for the more aromatized coal samples, which also implies greater microcrystalline ductility and stacking. The bituminous coal samples in this study contain a low degree of ordered microcrystalline units with a low degree of aromatic conformation.

Table 2 XRD structure parameters

Sample	d_{002}(Å)	f_a	L_c (Å)	L_a (Å)
SBPH	3.52	0.69	20.51	26.61
TFXQ	3.40	0.73	25.88	27.93
TFDX	3.42	0.62	17.27	25.78
YMXY	3.49	0.91	23.33	26.49

3.3 Raman spectroscopy analysis

Fig. 3 shows the Raman spectrum of the first-order mode range (1000-2000 cm^{-1}) after baseline correction.

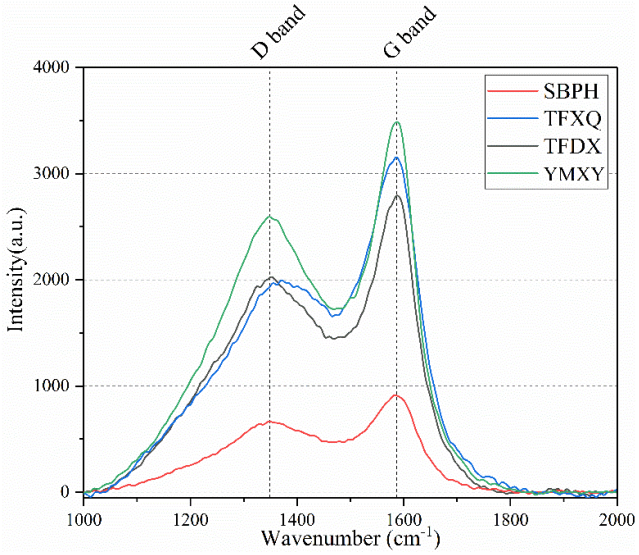

Fig. 3 The Raman spectra of four coal samples

Two distinct Raman frequency vibration regions can be clearly seen, that is, D band located near 1350 cm^{-1} and G band near 1590 cm^{-1}. Due to the overlap between D and G bands, the use of only D

and G bands in Raman spectroscopy will result in the loss or neglect of information about the properties of highly disordered carbonaceous materials [29]. Therefore, further integration of the Raman spectrum of the coal (peak fitting) is needed to obtain the hidden information of the skeleton carbon structure in the overlapping region. The method of Sadezky et al. [30] was used to solve this problem.

Take the TFXQ sample as an example, the Raman spectrum data obtained from the experiment was smoothed and the peak fitting was performed firstly. It was found in the result that the combination of four Lorentz peaks (D_1, D_2, D_4, G) located near 1360, 1620, 1180, and 1580cm^{-1} and a Gaussian peak (D_3) near 1500cm^{-1} were the most suitable and the fitting result is shown in Fig. 4. Based on the findings related to natural graphite and Raman spectra this show the carbonaceous material, a carbon atom with double stretching vibration peaking at G. This relates to the molecular structure, with vibration attributable to the aromatic E_{2g2} plane. D_1 relates to C-C bond peak vibrations between the aromatic ring and at least a 6 ring aromatic compound. The mode of vibration is attributable to the amorphous graphite A_{1g} irregular hexagonal lattice structure, defect intermolecular structural units and Heteroatom-related [30-33].

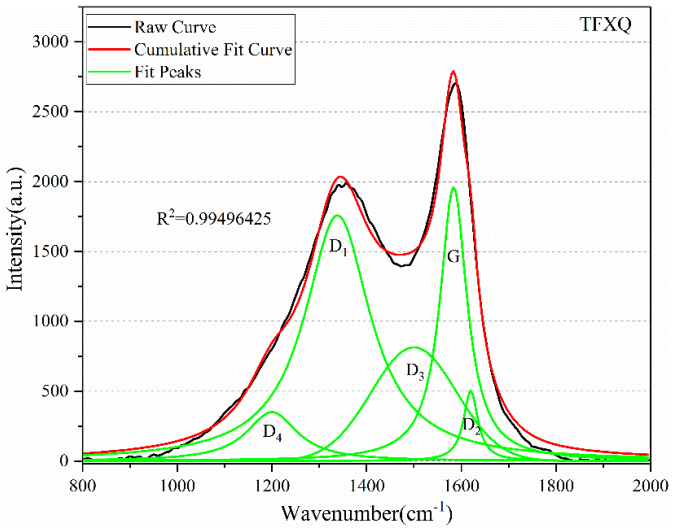

Fig. 4 Raman spectrum of TFXQ coal with the corresponding curve fitted bands

Positions of G peak and D_1 peak, difference of peak position (G-D1), and integrated intensity ratio (I_{D1}/I_G) and other characteristic parameters are important parameters for evaluating the degree of crystallinity or degree of defects in carbonaceous materials. The output data is shown in Table 3. It can be seen from Table 3 that the peak positions of the G and D_1 peaks of the four coal samples are

relatively close, and they are distributed near 1583 cm^{-1} and 1335 cm^{-1}, which indicates that the ordered structures in the four coal samples were similar. The range of G-D_1 is 245.06 – 249.63cm^{-1}. Its value of G-D_1 is higher than that of anthracite [42]. The peak position difference of the SBPH coal sample is the largest of the four, indicating that the coal sample has less disordered structure than other coal samples [34]. The range of I_{D1} / I_G is 2.18 ~ 2.48, among which the value of SBPH coal is significantly larger, indicating that its degree of graphitization is the lowest. On the contrary, the TFXQ coal sample has a better graphitization structure [16]. It is reported that as the coal metamorphism temperature increases, the G zone becomes the main zone, and the D zone gradually disappears, indicating that the structure of anthracite contact metamorphic coal is close to well-crystallized graphite [35]. The value of I_{D1} / I_G for bituminous coal is higher than that for anthracite [42], which also means that bituminous coal is less graphitized than anthracite. Therefore, bituminous coal has a lower combustion calorific value than anthracite, and has few advantages in combustion applications. The value of L_a ranges from 18.16 to 20.64, which is lower than the value calculated by XRD.

Table 3 Peak fitting parameters of Raman spectra of four coal samples

Sample	Peak	Position(cm^{-1})	Intensity	FWHM	G-D_1	I_{D1}/I_G	L_a (Å)
SBPH	G	1582.99	102800.00	69.46	249.63	2.48	18.16
	D_1	1333.36	254500.00	177.78			
TFXQ	G	1583.65	21400.00	69.42	245.06	2.18	20.64
	D_1	1338.59	466200.00	168.66			
TFDX	G	1583.62	120700.00	70.51	248.45	2.31	19.43
	D_1	1335.16	279300.00	180.83			
YMXY	G	1583.24	237700.00	69.66	247.82	2.37	18.95
	D_1	1335.42	564000.00	175.55			

3.4 FTIR spectra analysis

The FTIR spectra of the four groups of coal samples are shown in Figure 5.

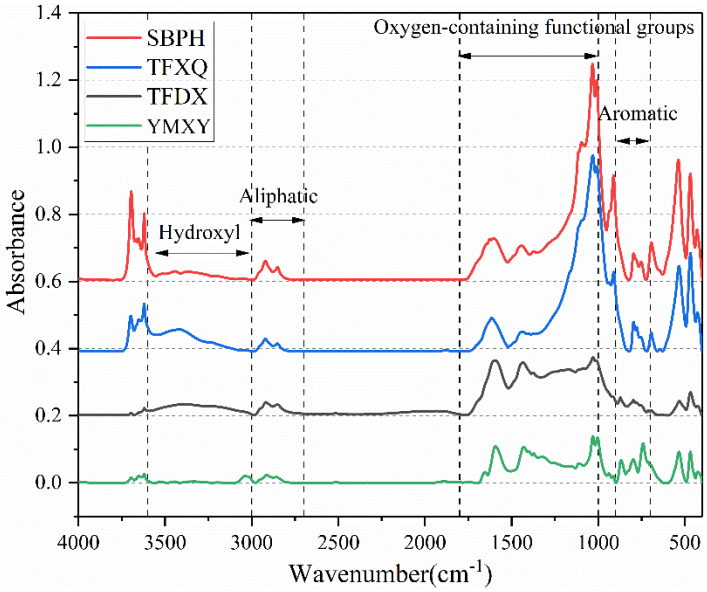

Fig.5 FTIR spectra of four coal samples

According to prior research, the main functional groups of coal include hydroxyl, aromatic, aliphatic and oxygen-containing functional groups. Their approximate range is shown in Figure 5. The hydroxyl and aliphatic absorption peak, the oxygen-containing functional group absorption peak and the aromatic structure absorption peak are located at 3600~3000 cm^{-1}, 3000~2700 cm^{-1}, 1800~1000 cm^{-1} and 900~700 cm^{-1} in the FTIR spectra, respectively. Specific peaks corresponding to the functional group are listed in Table 4.

Table 4 Corresponding assignment table of characteristic peaks of FTIR spectra [36-38]

Number	Peak position	Wavenumber range	Functional group assignment
1	3680	3685-3600	free -OH
2	3550	3600-3500	-OH self-contained hydrogen bond
3	3400	3550-3200	-OH stretching vibration
4	2950	2975-2950	CH_3 asymmetric stretching vibration
5	2920	2935-2915	CH_2 asymmetric stretching vibration
6	2870	2875-2860	CH_3 symmetric stretching vibration
7	2850	2860-2840	CH_2 symmetric stretching vibration
8	1750	1770-1800	Aliphatic C = O stretching vibration
9	1700	1715-1690	Aromatic C = O stretching vibration
10	1675	1690-1660	C = O stretching vibration in quinone
11	1600	1605-1595	Aromatic C = C stretching vibration
12	1470	1480-1465	CH_2 asymmetric deformation vibration
13	1440	1460-1435	CH_3 asymmetric deformation vibration
14	1380	1385-1370	CH_3 symmetric bending vibration
15	1150	1160-1120	C-O-C stretching vibration
16	1110	1120-1080	S = O stretching vibration

17	1050	1060-1020	Si-O-Si or Si-O-C stretching vibration
18	870	900-850	aromatic nucleus (CH), one adjacent H deformation
19	820	825-800	aromatic nucleus (CH), three adjacent H deformation
20	750	770-730	aromatic nucleus (CH), five adjacent H deformation
21	720	724-716	n-Alkane side chain skeleton $(CH_2)n$ oscillatory vibration

3.3.1 Qualitative analysis

Due to the condition of multiple peaks superimposed in the original image, the image needs to be deconvolved by Origin2017 to fit the specific functional group absorption peak information. By fitting the peaks in different regions, we can obtain information on different kinds of functional groups. The absorption peaks in the range of 3700-3000 cm^{-1} are predominantly hydroxyl. The absorption peaks of the samples are concentrated in the 3700-3600 cm^{-1} range, so there is a lot of free OH, which in turn can be judged to be likely to contain alcohols, phenols and organic acids [36]. The absorption peaks in the range of 3000-2700 cm^{-1} are aliphatic structures. Significant absorption peaks can be seen to be fitted at the peaks at 2950, 2920, 2870, 2850 cm^{-1}, and they correspond to the CH_3 asymmetric stretching vibration, CH_2 asymmetric stretching vibration, CH_3 symmetric stretching vibration and CH_2 symmetric stretching vibration, respectively.

3.3.1.1 Fitting analysis of 1800-1000cm^{-1} area

FTIR fitting curves for the absorption peaks in the range of 1800-1000 cm^{-1} for SBPH and YMXY coal samples are shown in Figure 6. Most of the absorption peaks in this range are oxygen-containing functional groups. The absorption peaks of the three groups of bituminous coal samples, were similar in shape, with larger absorption in the 1100-1000 cm^{-1} range and somewhat sharp shapes. This indicates the presence of more S=O telescopic vibrations, Si-O-Si or Si-O-C telescopic vibrations. Moreover, the four sets of samples showed significant peaks at 1600 and 1440 cm^{-1}, so that the presence of aromatic C=C stretching vibrations and CH_3 asymmetric deformation vibrations could be judged. A smaller absorption peak at 1700 cm^{-1}, a C=O stretching vibration in the aromatics, was also observed by fitting the curve.

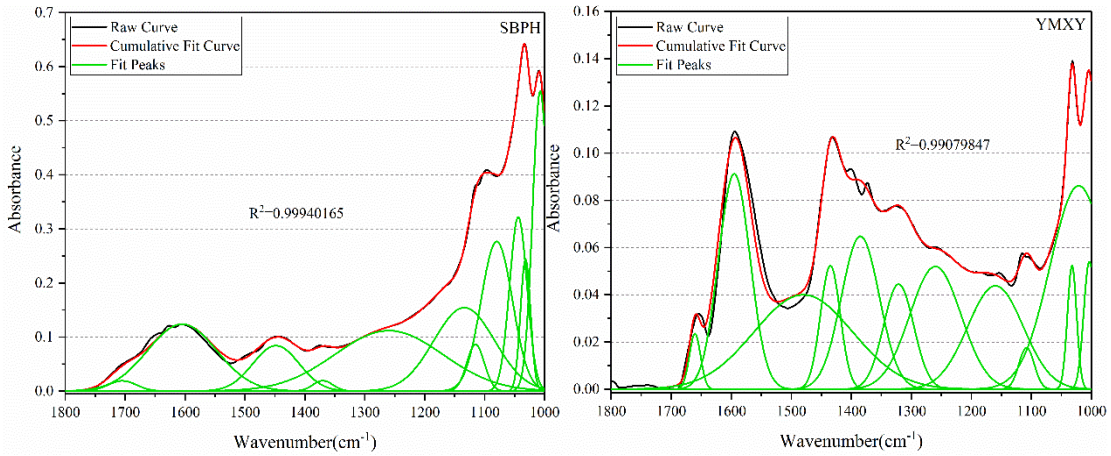

Fig. 6. 1800–1000 cm^{-1} FTIR spectra fitting curve of SBPH and YMXY

3.3.1.2 Fitting analysis of 900-700cm^{-1} area

FTIR fitting curves for the absorption peaks in the range of 900-700 cm^{-1} for SBPH and YMXY coal samples are shown in Figure 7. The absorption area in the wavenumber range of 900-700 cm^{-1} is mainly formed by the bending vibrations of poly-substituted aromatics. The absorption peaks of the SBPH coal sample is concentrated in the 900-800cm^{-1} wavelength range, suggesting that it contains mainly benzene ring structures in which individual H atoms are replaced by CH. While the absorption peaks of YMXY sample, is more uniformly distributed in the 900-700 cm^{-1} wavelength range, reflecting the benzene ring structure with a single H atom, three adjacent H atoms and five adjacent H atoms replaced by CH, and the n-alkane side chain backbone (CH_2) structure.

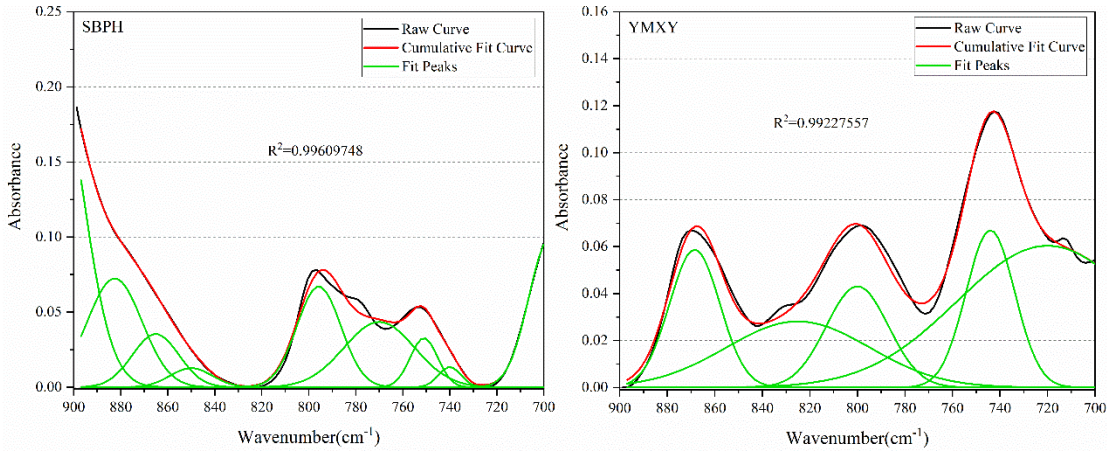

Fig. 7 900–700 cm^{-1} FTIR spectra fitting curve of SBPH and YMXY

3.3.2 Quantitative analysis

After determining the functional group, the area of its absorption peak can be obtained, and then the parameters of aromaticity fa, (R/C)u and CH_2/CH_3 can be calculated by Eqs.(10-15). Areas of absorption peaks of major functional groups in FTIR spectra are shown in Table 5. The proportion of hydroxyl groups, aliphatic groups, oxygenated functional groups and aromatic groups can be obtained by area normalization and the results are shown in Figure 8. It can be seen from the figure that the commonality of the three groups of bituminous coal (medium rank coal) samples is a large proportion of oxygen-containing functional groups and aromatic groups but lower than those of anthracite [42]. In addition, the hydroxyl content of bituminous coal (medium rank coal) is also higher than that of anthracite. Most of the oxygen-containing functional groups are hydrophilic groups that are easy to combine with hydrophilic substances, thereby forming composite materials with other impurities in bituminous coal, so they may be made into filters to treat wastewater [39].

Table 5 Area of absorption peaks of major functional groups in FTIR spectra

Sample	Hydroxyl groups	Aliphatic groups	Oxygen-containing functional groups	Aromatic groups
SBPH	17.12	13.67	46.12	26.91
TFXQ	23.98	8.87	19.25	24.58
TFDX	14.06	20.16	38.32	28.05
YMXY	1.96	9.60	14.00	12.86

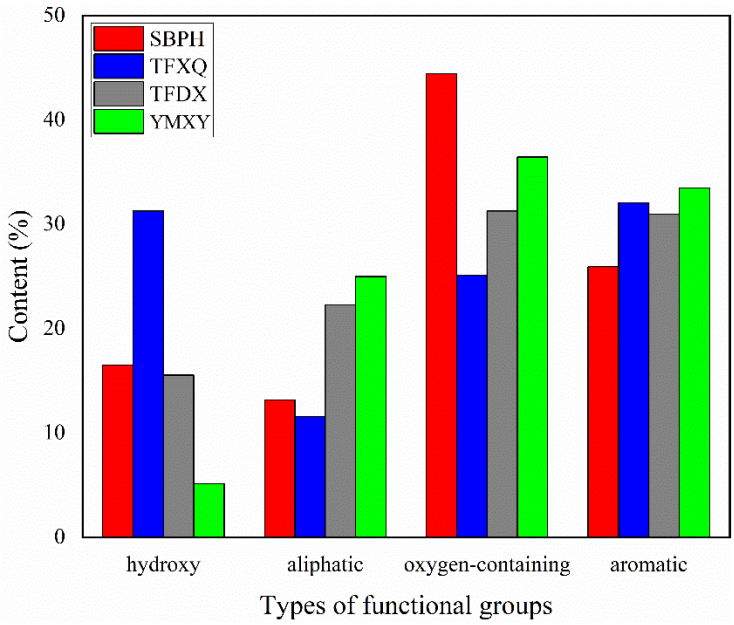

Fig.8 Proportion of different functional groups

Based on a simple understanding of the functional group occupancy, aromatic fa, lipid hydrogen

ratio Hal/H, single carbon ring number (R/C)u and aliphatic structural parameter CH_2/CH_3 can be obtained by Eqs. (10-15). The results are shown in Table 6.

Table 6 Molecular structure parameters of four bituminous coal samples obtained by FTIR method

Sample	H/C	Hal/H	Cal/C	f_a	(R/C)u	$A(CH_2)/A(CH_3)$
SBPH	0.88	0.60	0.29	0.71	0.21	0.32
TFXQ	0.88	0.34	0.17	0.83	0.14	0.18
TFDX	0.85	0.72	0.34	0.66	0.25	0.13
YMXY	0.54	0.52	0.16	0.84	0.31	0.13

Among them, f_a and (R/C)u reflect the information of aromatic structure in the macromolecular structure of coal to a certain extent, so as to judge the degree of aromatization of coal. CH_2/CH_3 reflects the length of aliphatic side chains in coal [37-38]. These parameters are an important basis for analysing the influence of coal molecular structure on its physical properties. It can be seen from Table 6 that the f_a of two coal samples of TFXQ and YMXY is larger than that of the other two coal samples, indicating that these two coal samples have a higher degree of aromatization [40-41]. However, although the f_a of the TFXQ coal sample is relatively large, its single carbon ring number (R/C)u is relatively small. Contrary to f_a, Hal/H reflects the higher content of aliphatic structure in the two coal samples of TFDX and SBPH than the other two coal samples. CH_2/CH_3 reflects that SBPH coal-like macromolecules have longer aliphatic side chains. Comparing the parameters of these three groups of bituminous coal samples with the anthracite samples [42], we can find that their f_a is lower than that of the anthracite, so the bituminous coal has a lower degree of aromatization than anthracite. In addition, its CH_2/CH_3 value is lower than that of high rank coal, so the aliphatic side chains of bituminous coal are shorter.

4. Conclusions

In this study, the molecular structure of bituminous coal and sub-bituminous coal was investigated using three methods, X-ray diffraction, Raman spectroscopy and Fourier Transform Infrared spectroscopy. From the qualitative and quantitative analysis of industrial analysis and spectroscopic test results, the conclusions are as follows:

(1) The results of industrial analysis show that the water content of different coal samples varied greatly, with the values ranging from 3.03 to 15.12%. The results of elemental analysis show that the

elemental content of bituminous coal was dominated by C elements, followed by O and H elements, with N and S elements accounting for a very small proportion.

(2) The results of the XRD analysis suggest that the bituminous coal samples in this study contain a low degree of ordered microcrystalline units with a low degree of aromatic conformation.

(3) The analysis of the Raman spectroscopy results shows that the peak difference G-D_1 is the largest in the SBPH coal sample (sub-bituminous coal), indicating that the disordered structure is less in this sample than in other bituminous coal samples. And generally bituminous coal has less disordered structure than anthracite. The I_{D1}/I_G of the TFXQ coal samples are significantly smaller, indicating that the degree of graphitization is higher. The value of I_{D1}/I_G for bituminous coal is higher than for high rank coal, which means that medium rank coal is less graphitized than high rank coal. Therefore, bituminous coal has a lower combustion calorific value than anthracite, and has few advantages in combustion applications.

(4) FTIR experimental analysis shows that the absorption peak areas of the oxygen-containing functional groups in the samples are generally the largest, followed by the aromatic structure, the aliphatic structure and the hydroxyl functional group with relatively small absorption peak areas. In addition, the molecular structure parameters obtained from the analysis indicate that the YMXY coal sample has a high degree of aromatization. The bituminous coal samples have a high content of aliphatic structure, and the SBPH coal sample has a long aliphatic side chain in the macromolecule. Parameter f_a of the bituminous coal is lower than that of the anthracite, so it has a lower degree of aromatization. Due to the large amount of oxygen-containing functional groups in bituminous coal, it has high hydrophilicity and can be used for adsorption and filtration

Notes

The authors declare that we do not have any commercial or associative interest that represents a conflict of interest in connection with the work submitted.

Acknowledgements

The authors are grateful to the Fundamental Research Funds for the National Natural Science Foundation of China (No. 51874298; No. 51804201), the Priority Academic Program Development of Jiangsu Higher Education Institutions (PAPD) and the University Cyan Project of the Jiangsu Province.

Nomenclature

f_a	the ratio of aromatic carbon to total carbon
d_{002}	inter-layer spacing (Å)
L_a	the average diameter of coal crystallites (Å)
L_c	the average height of coal crystallites (Å)
φ	peak position of XRD spectra (°)
λ	X-ray wavelength (Å)
λ_L	the wavelength of Raman laser (Å)
θ	the diffraction angle of X-ray (°)
C_{al}/H_{al}	the atomic ratio between C and H in aliphatic groups
C_{al}/C	the aliphatic carbon fraction
$(R/C)_u$	the number of rings of aromatic carbon in the monomer
H_{al}/H	the ratio of aliphatic (H_{al}) to the total hydrogen atoms (H)
$A(CH_2)/A(CH_3)$	the length of aliphatic chains or the degree of branching aliphatic side-chains

References

[1] Kejiang Li, Rita Khanna, Jianliang Zhang, Mansoor Barati, Zhengjian Liu, Tao Xu, Tianjun Yang, Veena Sahajwalla. Comprehensive Investigation of various structural features of bituminous coals using advanced analytical techniques. Energy & Fuels, 29 (2015) 7178-7189.

[2] Mustafa Baysal, Alp Yürüm, Burçin Yıldız, Yuda Yürüm. Structure of some western Anatolia coals investigated by FTIR, Raman, ^{13}C solid state NMR spectroscopy and X-ray diffraction. International Journal of Coal Geology, 163 (2016) 166–176.

[3] Gregory N. Okolo, Hein W.J.P. Neomagus, Raymond C. Everson, Mokone J. Roberts, John R. Bunt John R. Bunt, Jonathan P. Mathews. Chemical–structural properties of South African bituminous coals: Insights from wide angle XRD–carbon fraction analysis, ATR–FTIR, solid state ^{13}C NMR, and HRTEM techniques. Fuel, 158 (2015) 779-792.

[4] L. Cartz, P. B. Hirsch, A contribution to the structure of coals from x-ray diffraction studies. Philosophical transactions of the royal society of London. 252(1960)557-602.

[5] Meifen Li, Fangui Zeng, Haizhou Chang, Bingshe Xu, Wei Wang, Aggregate structure evolution of low-rank coals during pyrolysis by in-situ X-ray diffraction. International Journal of Coal Geology, 116-117 (2013) 262-269.

[6] Jingchong Yan, Zhiping Lei, Zhanku Li, Zhicai Wang, Shibiao Ren, Shigang Kang, Xiaoling Wang, Hengfu Shui, Molecular structure characterization of low-medium rank coals via XRD, solid state ^{13}C NMR and FTIR spectroscopy, Fuel, 268 (2020) 117038.

[7] Barbara Kwiecińska, Sławomira Pusz, Brett J. Valentine. Application of electron microscopy TEM and SEM for analysis of coals, organic-rich shales and carbonaceous matter. International Journal of Coal Geology, 211 (2019) 103203.

[8] Mengjie Liu, Jin Bai, Jianglong Yu, Lingxue Kong, Zongqing Bai, Huaizhu Li, Chong He, Zefeng Ge, Xi Cao, Wen Li, Correlation between char gasification characteristics at different stages and microstructure of char by combining x-ray diffraction and Raman spectroscopy. Energy & Fuels, 34(4) (2020) 4162-4172.

[9] Xiaoshi Li,Yiwen Ju , Quanlin Hou, Zhuo Li, FTIR and Raman spectral research on metamorphism

and deformation of coal. Journal of Geological Research, 2012 (2012) 1-8.
[10] Rajender Gupta. Advanced coal characterization: A review. Energy & fuels, 21(2) (2017) 451-460.
[11] André da S. Machado, André S. Mexias, Antonio C.F. Vilela, Eduardo Osorio, Study of coal, char and coke fines structures and their proportions in the off-gas blast furnace samples by X-ray diffraction. Fuel, 114 (2013) 224-228.
[12] Dangyu Song , Cunbei Yang, Xiaokui Zhang, Xianbo Su, Xiaodong Zhang, Structure of the organic crystallite unit in coal as determined by X-ray diffraction. Mining Science and Technology, 021(005) (2011) 667-671.
[13] Dun Wu, Guijian Liu, Ruoyu Sun, Shancheng Chen, Influences of magmatic intrusion on the macromolecular and pore structures of coal: Evidences from Raman spectroscopy and atomic force microscopy. Fuel, 119 (2014) 191-201.
[14] Morga, Rafa Jelonek, Iwona Kruszewska, Krystyna Szulik, Wojciech, Relationships between quality of coals, resulting cokes, and micro-Raman spectral characteristics of these cokes. International Journal of Coal Geology, 144–1451 (2015) 130-137.
[15] Sinha K, Menéndez, J. First- and second-order resonant Raman scattering in graphite. Physical Review B, 41(15) (1990) 10845-10847.
[16] Xiaojiang Li, Jun-ichiro Hayashi, Chun-zhu Li, FT-Raman spectroscopic study of the evolution of char structure during the pyrolysis of a Victorian brown coal. Fuel, 85(12/13) (2006) 1700-1707.
[17] Diane S. Knight, William B. White, Characterization of diamond films by Raman spectroscopy. Journal of Materials Research, 4(02) (1989) 385-393.
[18] GEORGAKOPOULOS, ANDREAS. Study of low rank Greek coals using FTIR spectroscopy. Energy Sources, 25(10) (2003) 995-1005.
[19] Yanyan Chen, Maria Mastalerz, Arndt Schimmelmann, Characterization of chemical functional groups in macerals across different coal ranks via micro-FTIR spectroscopy. International journal of coal geology, 104 (2012) 22-33.
[20] Manoj Balachandran. Role of Infrared spectroscopy in coal analysis-an investigation. American Journal of Analytical Chemistry, 5(6) (2014) 367-372.
[21] Kejiang Li, Rita Khanna, Jianliang Zhang, Mansoor Barati, Comprehensive investigation of various structural features of bituminous coals using advanced analytical techniques. Energy & fuels, 29 (2015) 7178-7189.
[22] B. Alpern, Coal. Typology-Physics-Chemistry-Constitution: by D.W. van Krevelen. Third, completely revised edition. Elsevier Science, Amsterdam, 1993. Harboound, xxi + 979 pp. US$ 397; ISBN 0-444-89586-8. International Journal of Coal Geology, 26(3-4) (1994) 261-262.
[23] J. Kastner, T. Pichler, H. Kuzmany, S. Curran, W. Blau, D.N. Weldon, M. Delamesiere, S. Draper, H. Zandbergen, Resonance Raman and infrared spectroscopy of carbon nanotubes. Chemical Physics Letters, 221(1-2) (1994) 53-58.
[24] Orrego-Ruiz J A, Cabanzo R, Enrique Mejía-Ospino. Study of colombian coals using photoacoustic Fourier transform infrared spectroscopy. international journal of coal geology, 85(3-4) (1994) 307-310.
[25] Noriko YOSHIZAWA, Katsuhisa MARUYAMA, Yoshio YAMADA, Yoshikazu TAKAHASHI, Gen KATAGIRI, Yukio SHIMANE, Michiaki HARADA, Standardization of carbon structural analysis in coal by X-ray diffraction (1) influence of deashing and solvent treatment upon stacking structure of aromatic layers in coal. Journal of the Japan Institute of Energy, 80 (2001) 343-349.

[26] The Fu. Yen, J. Gordon Erdman, S. S. Pollack, Investigation of the structure of petroleum asphaltenes by x-ray diffraction. Analytical Chemistry, 33(11) (1961) 1587-1594.
[27] Manyalibo Joseph Matthews, Marcos A Pimenta, G. Dresselhaus, M. S. Dresselhaus, Origin of dispersive effects of the raman d band in carbon materials. Physical Review B, 59(10) (1999) R6585–R6588.
[28] Yongshuai Fu, Xianfeng Liu, Boqing Ge, Zhenghong Liu, Role of chemical structures in coalbed methane adsorption for anthracites and bituminous coals. Adsorption, 23(5) (2017) 711-721.
[29] Matthew W. Smith, Ian Dallmeyer, Timothy J. Johnson, Carolyn S. Brauer, Jean-Sabin McEwen, Juan F. Espinal, Manuel Garcia-Perez, Structural analysis of Char by Raman spectroscopy: improving band assignments through first principle computational calculations. Carbon, 100 (2016) 678-692.
[30] A. Sadezky, H. Muckenhuber, H. Grothe, R. Niessner, U. Pöschl, Raman microspectroscopy of soot and related carbonaceous materials: Spectral analysis and structural information. Carbon, 43(8) (2005) 1731-1742.
[31] Olivier Beyssac, Bruno Goffé, Jean-Pierre Petitet, Emmanuel Froigneux, Myriam Moreau, Jean-Noël Rouzaud, On the characterization of disordered and heterogeneous carbonaceous materials by Raman spectroscopy. Spectrochimica Acta Part A Molecular & Biomolecular Spectroscopy, 59(10) (2003) 2267-2276.
[32] Jun Xu, Sheng Su, Zhijun Sun, Mengxia Qing, Zhe Xiong, Yi Wang, Long Jiang, Song Hu, Jun Xiang, Effects of steam and CO_2 on the characteristics of chars during devolatilization in oxy-steam combustion process, Applied Energy, 182 (2016) 20-28.
[33] T. Jawhari, A. Roid, J. Casado, Raman spectroscopic characterization of some commercially available carbon black materials. Carbon, 33(11) (1995) 1561-1565.
[34] S. R. Kelemen, H. L. Fang, Maturity trends in raman spectra from kerogen and coal. Energy & Fuels, 15(3) (2001)653-658.
[35] Shancheng Chen, Dun Wu, Guijian Liu, Ruoyu Sun, Raman spectral characteristics of magmatic-contact metamorphic coals from Huainan Coalfield, China. Spectrochimica Acta Part A: Molecular and Biomolecular Spectroscopy, 171 (2017) 31-39.
[36] Dun Wu, Guijian Liu, Ruoyu Sun, Fan Xiang, Investigation of structural characteristics of thermally metamorphosed coal by FTIR spectroscopy and X-ray diffraction. Energy & fuels, 27 (2013) 5823-5830.
[37] Painter, Paul C. Snyder, Randy W. Starsinic, Michael Coleman, Michael M. Kuehn, Deborah W. Davis, Alan, Concerning the application of FT-IR to the study of coal: A critical assessment of band assignments and the application of spectral analysis programs. applied spectroscopy, 35(5) (1981) 475-485.
[38] Paul Painter, Michael Starsinic, Michael Coleman, Determination of functional groups in coal by Fourier Transform Interferometry. Fourier Transform Infrared Spectra, (1985) 169-241.
[39] Hongxiang Xu, Research on Coal Adsorption Purification Mechanism for Organic Wastewater Treatment, Phd Thesis, China University of Mining and Technology,2015.
[40] R.M Bustin, Y Guo, Abrupt changes (jumps) in reflectance values and chemical compositions of artificial charcoals and inertinite in coals, International Journal of Coal Geology, 38(3–4) (1999) 237-260.
[41] Zhongsheng Li, Peter M. Fredericks, Llew Rintoul, Colin R. Ward, Application of attenuated total reflectance micro-Fourier transform infrared (ATR-FTIR) spectroscopy to the study of coal macerals:

503 Examples from the Bowen Basin, Australia. International Journal of Coal Geology, 70(1/3) (2007)
504 87-94.
505 [42] Jingyu Jiang, Weihua Yang, Yuanping Cheng, Zhengdong Liu, Qiang Zhang, Ke Zhao. Molecular
506 structure characterization of middle-high rank coal via XRD, Raman and FTIR spectroscopy:
507 Implications for coalification. Fuel, 239 (2019) 559-572.

Declaration of interests

The authors declare that they have no known competing financial interests or personal relationships that could have appeared to influence the work reported in this paper.